

Mixed-Metal Cluster Chemistry. 2.¹ Site-Selective Substitution of CpWIr₃(CO)₁₁ by Phosphines: X-ray Crystal Structures of CpWIr₃(μ-CO)₃(CO)₇(PPh₃), CpWIr₃(μ-CO)₃(CO)₆(PPh₃)₂, and CpWIr₃(μ-CO)₃(CO)₇(PMe₃)

Susan M. Waterman and Mark G. Humphrey*

Department of Chemistry, Australian National University, Canberra, ACT 0200, Australia

Vicki-Anne Tolhurst

Department of Chemistry, University of New England, Armidale, NSW 2351, Australia

Brian W. Skelton and Allan H. White

Department of Chemistry, University of Western Australia, Nedlands, WA 6907, Australia

David C. R. Hockless

Research School of Chemistry, Australian National University, Canberra, ACT 0200, Australia

Received July 20, 1995[⊗]

Reactions of CpWIr₃(CO)₁₁ (**1**) with stoichiometric amounts of phosphines afford site-selective products CpWIr₃(μ-CO)₃(CO)_{8-x}(L)_x (L = PPh₃, *x* = 1 (**2**), 2 (**3**), or 3 (**4**); L = PMe₃, *x* = 1 (**5**), 2 (**6**), or 3 (**7**)) in fair to excellent yields (38–63%). These products exhibit ligand fluxionality in solution, resolvable at low temperature into the constituent interconverting isomers. The structures of three of the species, namely **2a**, **3a**, and **5a**, have been determined by X-ray diffraction studies. The single-crystal X-ray studies reveal that ligand substitution induces a rearrangement in the cluster coordination sphere from the all-terminal carbonyl ligand geometry of CpWIr₃(CO)₁₁ to one in which the three edges of a WIr₂ face of the tetrahedral core contain bridging carbonyls (**2a**, **3a**) or one in which the three edges of the triiridium face are bridged by carbonyl ligands (**5a**). The triphenylphosphine in **2a** ligates radially to the carbonyl-bridged WIr₂ face; a similar site for one of the phosphines is found in **3a**, with the second triphenylphosphine coordinated in an axial position with respect to this face. The trimethylphosphine ligand in **5a** is located in an axial site with respect to the basal carbonyl-bridged triiridium plane. Information from the crystallographically-verified isomers, the ligand substitution pattern in the related tetrairidium system, and chemical shifts of signals in the ³¹P NMR spectra has been used to suggest coordination geometries for the isomeric forms of the complexes above and for other reported derivatives.

Introduction

The chemistry of mixed-metal clusters has been the subject of great interest.² Although site selectivity investigations of mixed-metal clusters with phosphines have been widespread,^{2a,3} most of these studies have been with mixed-metal clusters containing metals from the same group or from adjacent groups.

Results from work with tetrahedral clusters have been summarized.^{3j} Although the least sterically hindered sites are the radial carbonyl sites (Figure 1), most

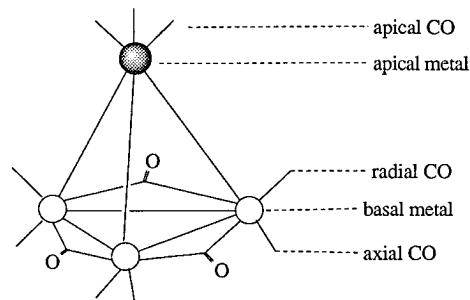


Figure 1.

monosubstituted homometallic or pseudotetrahedral heterometallic clusters have ligands in an axial site, presumably an electronic effect. Homometallic cluster substitution then proceeds at a different basal metal to afford bis-substituted derivatives with diaxial coordination for small ligands or radial, axial coordination for sterically encumbered ligands. The third incoming ligand occupies a basal coordination site to minimize

* To whom correspondence should be addressed.

⊗ Abstract published in *Advance ACS Abstracts*, January 15, 1996.

(1) Part 1: Lee, J.; Humphrey, M. G.; Hockless, D. C. R.; Skelton, B. W.; White, A. H. *Organometallics* **1993**, *12*, 3457.

(2) (a) Gladfelter, W. L.; Fox, J. R.; Smegal, J. A.; Wood, T. G.; Geoffroy, G. L. **1981**, *20*, 3223. (b) Roberts, D. A.; Geoffroy, G. L. In *Comprehensive Organometallic Chemistry*; Wilkinson, G., Stone, F. G. A., Abel, E. W., Eds.; Pergamon Press: Oxford, U.K., 1982; Vol. 6, p 763. (c) Bruce, M. I. *J. Organomet. Chem.* **1983**, *242*, 147. (d) Bruce, M. I. *J. Organomet. Chem.* **1985**, *17*, 399. (e) Sappa, E.; Tiripicchio, A.; Braunstein, P. *Coord. Chem. Rev.* **1985**, *65*, 219.

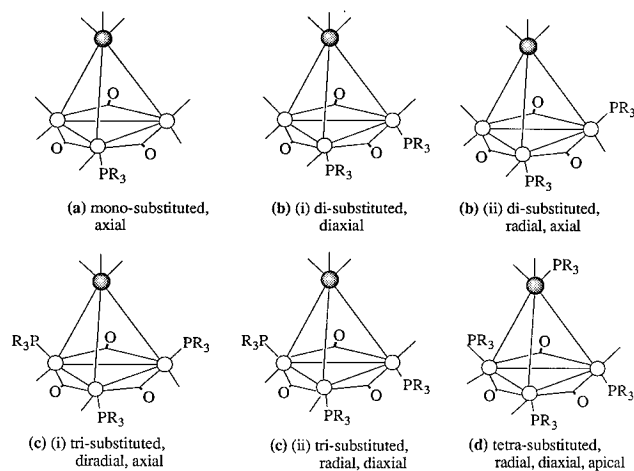


Figure 2. Common substitution geometries for tetrahedral clusters with edge-bridging carbonyls about one face.

steric effects, to usually give a diradial, axial derivative. The fourth ligand substitutes at the apical metal, forcing the two ligands of the basal metals on the $M_{\text{apical}}(M_{\text{basal}})_2$ face to axial sites and the other ligand into a radial site (Figure 2). For mixed-metal hydrido clusters of this geometry, the hydride occupies a face-capping site below the basal plane, displacing the radial carbonyls toward the apical metal and increasing available space at the axial site; both mono- and disubstitution are commonly axial.

By contrast with the studies above, investigations with mixed-metal clusters employing widely differing metals are comparatively rare. We have previously reported site-specific products from reaction between $\text{CpWIr}_3(\text{CO})_{11}$ (**1**) and equimolar PPh_3 , dppm , dppe , or dppa and structural studies on $\text{CpWIr}_3(\mu\text{-L})(\mu\text{-CO})_3(\text{CO})_6$ ($\text{L} = \text{dppm}, \text{dppe}, \text{dppa}$).¹ We report herein the reactivity of **1** toward 1, 2, or 3 equiv of PPh_3 or PMe_3 and the characterization by single-crystal X-ray studies of three of the site-selective reaction products, $\text{CpWIr}_3(\mu\text{-CO})_3(\text{CO})_7(\text{PPh}_3)$ (**2a**), $\text{CpWIr}_3(\mu\text{-CO})_3(\text{CO})_6(\text{PPh}_3)_2$ (**3a**), and $\text{CpWIr}_3(\mu\text{-CO})_3(\text{CO})_7(\text{PMe}_3)$ (**5a**).

Experimental Section

General Information. All reactions were performed under an atmosphere of dry nitrogen (high-purity grade, CIG),

(3) (a) Lindsell, W. E.; Walker, N. M.; Boyd, A. S. F. *J. Chem. Soc., Dalton Trans.* **1988**, 675. (b) Pursiainen, J.; Ahlgren, M.; Pakkanen, T.; Valkonen, J. *J. Chem. Soc., Dalton Trans.* **1990**, 1147. (c) Curnow, O. J.; Kampf, J. W.; Curtis, M. D. *Organometallics* **1991**, *10*, 2546. (d) Ojima, I.; Clos, N.; Donovan, R. J.; Ingallina, P. *Organometallics* **1991**, *10*, 3211. (e) Le Grand, J.-L.; Lindsall, W. E.; McCullough, K. J. *J. Organomet. Chem.* **1991**, *413*, 321. (f) Le Grand, J.-L.; Lindsall, W. E.; McCullough, K. J.; McIntosh, C. H.; Meiklejohn, A. G. *J. Chem. Soc., Dalton Trans.* **1992**, 1089. (g) Fox, J. R.; Gladfelter, W. L.; Wood, T. G.; Smegal, J. A.; Foreman, T. K.; Geoffroy, G. L.; Tavaniaiepour, I.; Day, V. W.; Day, C. S. *Inorg. Chem.* **1981**, *20*, 3214. (h) Horvath, I. T. *Organometallics* **1986**, *5*, 2333. (i) Sappa, E.; Marchino, M. L. N.; Predieri, G.; Tiripicchio, A.; Camellini, M. T. *J. Organomet. Chem.* **1986**, *307*, 97. (j) Bojczuk, M.; Heaton, B. T.; Johnson, S.; Ghilardi, C. A.; Orlandini, A. *J. Organomet. Chem.* **1988**, *341*, 473. (k) Pakkanen, T. A.; Pursiainen, J.; Venäläinen, T.; Pakkanen, T. T. *J. Organomet. Chem.* **1989**, *372*, 129. (l) Pursiainen, J.; Pakkanen, T. A. *Acta. Chem. Scand. Ser. A* **1989**, *43*, 463. (m) Matsuzaka, H.; Kodama, T.; Uchida, Y.; Hidaï, M. *Organometallics* **1988**, *7*, 1608. (n) Pursiainen, J.; Pakkanen, T. A.; Jääskeläinen, J. *J. Organomet. Chem.* **1985**, *290*, 85. (o) Bahsoun, A. A.; Osborn, J. A.; Voelker, C.; Bonnet, J. J.; Lavigne, G. *Organometallics* **1982**, *1*, 1114. (p) Eshtiagh-Hosseini, H.; Nixon, J. F. *J. Organomet. Chem.* **1978**, *150*, 129. (q) Labroue, D.; Queau, R.; Poilblanc, R. *J. Organomet. Chem.* **1980**, *186*, 101. (r) Huie, B. T.; Knobler, C. B.; Kaesz, H. D. *J. Am. Chem. Soc.* **1978**, *100*, 3059. (s) Le Grand, J.-L.; Lindsall, W. E.; McCullough, K. J. *J. Organomet. Chem.* **1989**, *373*, C1.

although no special precautions were taken to exclude air during workup. The reaction solvent dichloromethane was dried over CaH_2 , and tetrahydrofuran (THF) was distilled from sodium/benzophenone under argon prior to use; all other solvents were reagent grade and used as received. Petroleum ether refers to a fraction of boiling point range 40–70 °C. The products of thin-layer chromatography were separated on 20 × 20 cm glass plates coated with Merck GF₂₅₄ silica gel (0.5 mm). The clusters $\text{CpWIr}_3(\text{CO})_{11}$ ⁴ and $\text{CpWIr}_3(\mu\text{-CO})_3(\text{CO})_7(\text{PPh}_3)$ ¹ were prepared by the published procedures. Triphenylphosphine (Aldrich) and trimethylphosphine (Aldrich, 1 M solution in THF) were purchased commercially and used as received.

Physical Measurements. Infrared spectra were recorded on a Perkin-Elmer Model 1600 Fourier transform spectrophotometer with CaF_2 optics. ¹H and ¹³C NMR spectra were recorded on a Varian Gemini 300 spectrometer (¹H spectra at 300 MHz, ¹³C at 75 MHz). The ¹³C NMR spectra were proton decoupled and recorded using ca. 0.02 M $\text{Cr}(\text{acac})_3$ as a relaxation agent. ³¹P NMR spectra were recorded on a Varian VXR300S spectrometer (121 MHz) and are proton decoupled. Spectra were run in CDCl_3 (Aldrich) or acetone-*d*₆ (Aldrich); chemical shifts in ppm are referenced to internal residual solvent for ¹H and ¹³C NMR spectra and external 85% H_3PO_4 for ³¹P NMR spectra.

Mass spectra were obtained either at the University of Adelaide on a VG ZAB 2HF mass spectrometer (FAB source of argon at 10⁻⁶ mbar, FAB gun voltage 7.5 kV, current 1 mA, ion accelerating potential 8 kV, matrix 3-nitrobenzyl alcohol, ca. 0.5 M solutions in dichloromethane) or at the Australian National University on a VG ZAB 2SEQ instrument (30 kV Cs⁺ ions, current 1 mA, accelerating potential 8 kV, matrix 3-nitrobenzyl alcohol). Peaks were recorded as *m/z* based on ¹⁸³W assignments and are reported in the following form: *m/z* (assignment, relative intensity). Elemental microanalyses were performed by the Microanalysis Service Unit in the Research School of Chemistry, Australian National University, or by the Microanalysis Service Unit in the Department of Chemistry, University of Queensland. Decomposition temperatures and melting points were measured in sealed capillaries using a Gallenkamp melting point apparatus.

Reaction of $\text{CpWIr}_3(\text{CO})_{11}$ with 2 equiv of PPh_3 . An orange solution of $\text{CpWIr}_3(\text{CO})_{11}$ (30.3 mg, 0.0267 mmol) and PPh_3 (14.0 mg, 0.0534 mmol) in CH_2Cl_2 (20 mL) was stirred at room temperature for 24 h. The dark orange solution obtained was evaporated to dryness. The resultant orange residue was dissolved in CH_2Cl_2 (ca. 1 mL) and chromatographed (3:2 CH_2Cl_2 /petroleum ether eluant). Three bands were obtained. The contents of the first band were identified as $\text{CpWIr}_3(\mu\text{-CO})_3(\text{CO})_7(\text{PPh}_3)$ (**2.3** mg, 6%) by solution IR spectroscopy. The second band contained a small amount of an unidentified green compound. Crystallization of the contents of the third band, *R*_f 0.48, from CH_2Cl_2 /MeOH afforded orange crystals of $\text{CpWIr}_3(\mu\text{-CO})_3(\text{CO})_6(\text{PPh}_3)_2$, **3** (12.0 mg, 45%, mp 167 °C (dec)). Analytical data for **3**: IR (c-C₆H₁₂) 2059 vs, 2027 w, 2009 s, 2001 vs, 1986 s, 1958 m, 1904 m, 1815 m cm^{-1} ; ¹H NMR (CDCl_3) δ 7.58–7.29 (m, 30H, C₆H₅), 4.87 (s (br), 5H, C₅H₅); ¹³C NMR (CDCl_3) δ 133.9–128.0 (C₆H₅), 87.5 (C₅H₅); ³¹P NMR (CDCl_3) δ 27.3 (s, 2P), 25.1 (s, 1P), –7.7 (s, 1P); FAB MS 1602 ([M]⁺, 57), 1574 ([M – CO]⁺, 54), 1546 ([M – 2CO]⁺, 69), 1518 ([M – 3CO]⁺, 100), 1490 ([M – 4CO]⁺, 42), 1462 ([M – 5CO]⁺, 100), 1434 ([M – 6CO]⁺, 64), 1406 ([M – 7CO]⁺, 58), 1378 ([M – 8CO]⁺, 40). Anal. Calcd: C, 37.48; H, 2.20. Found: C, 37.44; H, 2.22%.

Reaction of $\text{CpWIr}_3(\text{CO})_{11}$ with 3 equiv of PPh_3 . An orange solution of $\text{CpWIr}_3(\text{CO})_{11}$ (21.5 mg, 0.0190 mmol) and PPh_3 (14.9 mg, 0.0568 mmol) in CH_2Cl_2 (25 mL) was stirred at room temperature for 18 h and then evaporated to dryness. The resultant dark orange residue was redissolved in CH_2Cl_2

(4) Shapley, J. R.; Hardwick, J.; Foose, D. S.; Stucky, G. D. *J. Am. Chem. Soc.* **1981**, *103*, 7383.

(ca. 1 mL) and chromatographed (3:2 CH₂Cl₂/petroleum ether eluant) to afford two products, one of which was in trace amounts. The major product, *R_f* 0.29, was crystallized (CHCl₃/EtOH at -20 °C) to afford red crystals of CpWIr₃(μ-CO)₃(CO)₅(PPh₃)₃, **4** (16.2 mg, 46%, mp 145 °C (dec)).⁵ Analytical data for **4**: IR (c-C₆H₁₂) 2059 m, 2027 w, 2009 s, 2000 vs, 1986 s, 1958 m, 1904 m, 1815 m cm⁻¹; ¹H NMR (acetone-*d*₆) δ 8.02 (s, 0.66H, CHCl₃), 7.57–7.37 (m, 45H, C₆H₅), 4.82 (s, 5H, C₅H₅); ³¹P NMR (CDCl₃) δ 31.8 (s, 2P), -17.9 (s, 1P); FAB MS 1420 ([M - PPh₃ - 2Ph]⁺, 43), 1392 ([M - PPh₃ - 2Ph - CO]⁺, 39), 1364 ([M - PPh₃ - 2Ph - 2CO]⁺, 100), 1336 ([M - PPh₃ - 2Ph - 3CO]⁺, 84), 1308 ([M - PPh₃ - 2Ph - 4CO]⁺, 58). Anal. Calcd: C, 42.42; H, 2.67. Found: C, 42.16; H, 2.38.

Reaction of CpWIr₃(CO)₁₁ with 1 equiv of PMe₃. An orange solution of CpWIr₃(CO)₁₁ (21.0 mg, 0.0185 mmol) and PMe₃ (20 μL, 1 M solution in THF, 0.020 mmol) in THF (20 mL) was stirred at room temperature for 18 h after which solvent was removed from the resulting dark orange solution *in vacuo*. The orange residue was dissolved in CH₂Cl₂ (ca. 1 mL) and chromatographed (3:2 CH₂Cl₂/petroleum ether eluant) to afford two products, one of which was in trace amounts. The major product, *R_f* 0.19, was crystallized (CHCl₃/MeOH) to afford orange crystals of CpWIr₃(μ-CO)₃(CO)₇(PMe₃)₃, **5** (8.2 mg, 38%, mp 143 °C). Analytical data for **5**: IR (c-C₆H₁₂) 2070 s, 2040 vs, 2030 m, 2021 s, 2003 s, 1992 vs, 1958 w, 1920 m, 1840 w cm⁻¹; ¹H NMR (CDCl₃) δ 5.03 (s, 5H, C₅H₅), 1.91 (d, *J*_{HP} = 11 Hz, 6H, CH₃); ¹³C NMR (acetone-*d*₆) δ 84.0 (s, C₅H₅), 20.4 (d, *J*_{CP} = 38 Hz, CH₃), 20.1 (s, CH₃); ³¹P NMR (acetone-*d*₆) δ -26.1 (s, 1P), -30.2 (s, 1P); FAB MS 1182 ([M]⁺, 6), 1154 ([M - CO]⁺, 38), 1126 ([M - 2CO]⁺, 42), 1098 ([M - 3CO]⁺, 69), 1070 ([M - 4CO]⁺, 100), 1042 ([M - 5CO]⁺, 31), 1028 ([M - 5CO - CH₃]⁺, 10), 1012 ([M - 5CO - 2CH₃]⁺, 55), 997 ([M - 5CO - 3CH₃]⁺, 11), 984 ([M - 6CO - 2CH₃]⁺, 46), 969 ([M - 6CO - 3CH₃]⁺, 32), 954 ([M - 6CO - 4CH₃]⁺, 15). Anal. Calcd: C, 18.29; H, 1.19. Found: C, 18.24; H, 0.80.

Reaction of CpWIr₃(CO)₁₁ with 2 equiv of PMe₃. An orange solution of CpWIr₃(CO)₁₁ (22.9 mg, 0.0203 mmol) and PMe₃ (40 μL, 1 M solution in THF, 0.040 mmol) in THF (20 mL) was stirred at room temperature for 18 h, after which the solvent was removed from the dark orange solution *in vacuo*. The resultant orange residue was dissolved in CH₂Cl₂ (ca. 1 mL) and chromatographed (3:2 CH₂Cl₂/petroleum ether eluant) to afford two products, one of which was in trace amounts. The major product, *R_f* 0.40, was crystallized (CHCl₃/MeOH) to afford orange crystals of CpWIr₃(μ-CO)₃(CO)₆(PMe₃)₂, **6** (9.6 mg, 41%, 159 °C). Analytical data for **6**: IR (c-C₆H₁₂) 2044 m, 2004 vs, 1988 vs, 1977 m, 1965 m, 1955 m, 1807 w cm⁻¹; ¹H NMR (CDCl₃) δ 5.06 (s, 5H, C₅H₅), 1.97 (d, *J*_{HP} = 10 Hz, 3H, CH₃); ¹³C NMR (acetone-*d*₆) δ 88.3 (s, C₅H₅), 20.5 (d, *J*_{CP} = 38 Hz, CH₃), 20.3 (s, CH₃); ³¹P NMR (acetone-*d*₆) δ -20.8 (s, 2P), -22.7 (s, 1P), -38.7 (s, 1P); FAB MS 1202 ([M - CO]⁺, 12), 1174 ([M - 2CO]⁺, 24), 1146 ([M - 3CO]⁺, 100), 1118 ([M - 4CO]⁺, 37), 1090 ([M - 5CO]⁺, 14), 1062 ([M - 6CO]⁺, 37), 1034 ([M - 7CO]⁺, 23). Anal. Calcd: C, 19.55; H, 1.89. Found: C, 19.49; H, 1.91.

Reaction of CpWIr₃(CO)₁₁ with 3 equiv of PMe₃. An orange solution of CpWIr₃(CO)₁₁ (22.3 mg, 0.0198 mmol) and PMe₃ (60 μL, 1 M solution in THF, 0.060 mmol) in THF (20 mL) was stirred at room temperature for 18 h, after which the solvent was removed from the dark orange solution *in vacuo*. The resultant orange residue was dissolved in CH₂Cl₂ (ca. 1 mL) and chromatographed (3:2 CH₂Cl₂/petroleum ether eluant) to afford one product. The orange band, *R_f* 0.56, was crystallized (CHCl₃/MeOH) to afford orange crystals of CpWIr₃(μ-CO)₃(CO)₅(PMe₃)₃, **7** (8.2 mg, 63%). Analytical data for **7**: IR (c-C₆H₁₂) 2002 s, 1966 vs, 1957 s, 1949 vs, 1815 vw cm⁻¹; ¹H NMR (CDCl₃) δ 4.89 (s, 5H, C₅H₅), 1.54 (d, *J*_{HP} = 10 Hz, 9H, CH₃); ³¹P NMR (CDCl₃) δ -27.1 (s, 1P), -45.2 (s, 1P), -83.4 (s, 1P); FAB MS 1222 ([M - 2CO]⁺, 80), 1194 ([M -

Table 1. Crystallographic Data for 2a, 3a, and 5a

	2a	3a	5a
chem formula	C ₃₃ H ₂₀ Ir ₃ O ₁₀ PW	C ₅₀ H ₃₅ Ir ₃ O ₉ P ₂ W	C ₁₈ H ₁₄ Ir ₃ O ₁₀ PW
fw	1367.9	1602.2	1181.8
space group	<i>P</i> $\bar{1}$ (No. 2)	<i>P</i> 2 ₁ / <i>c</i> (No. 14)	<i>P</i> $\bar{1}$ (No. 2)
cryst system	triclinic	monoclinic	triclinic
<i>a</i> , Å	15.174(7)	15.262(3)	9.486(2)
<i>b</i> , Å	11.792(4)	10.808(5)	17.058(4)
<i>c</i> , Å	9.774(5)	28.92(2)	30.590(6)
α, deg	79.33(4)		100.08(2)
β, deg	83.28(4)	98.38(5)	94.60(2)
γ, deg	78.77(3)		89.63(2)
<i>V</i> , Å ³	1680	4720	4857
ρ _{calcd} , g cm ⁻³	2.70	2.25	3.231
<i>Z</i>	2	4	8
μ, mm ⁻¹	15.4	11.0	21.3
spec size, mm	0.084 × 0.45 × 0.12	0.064 × 0.037 × 0.18	0.22 × 0.10 × 0.16
<i>A</i> * (min, max)	3.2, 6.5	1.3, 1.9	1, 3.2
2θ _{max} , deg	60	50	50
<i>N</i>	9805	8283	17 219
<i>N</i> _o	7362	3068	8921
<i>R</i>	0.043	0.071	0.039
<i>R</i> _w ^a	0.049 ^b	0.070 ^b	0.034 ^c

^a $R_w(F_o) = (\sum w(|F_o| - |F_c|)^2 / \sum w F_o^2)^{1/2}$. ^b Statistical weights derivative of $\sigma^2(I) = \sigma^2(I_{\text{diff}}) + 0.0004\sigma^4(I_{\text{diff}})$; useful data were limited in consequence of specimen size, supporting meaningful anisotropic thermal parameter refinement for Ir, W, and P only. ^c $w = 4F_o^2 / \sigma^2(F_o^2)$, where $\sigma^2(F_o^2) = [\sigma^2(C + 4B) + (pF_o^2)^2] / Lp^2$ (s = scan rate, C = peak count, B = background count, p = 0.007 determined experimentally from standard reflections).

3CO]⁺, 75), 1166 ([M - 4CO]⁺, 100), 1138 ([M - 5CO]⁺, 45), 1110 ([M - 6CO]⁺, 80), 1082 ([M - 7CO]⁺, 40), 1067 ([M - 7CO - CH₃]⁺, 50), 1052 ([M - 7CO - 2CH₃]⁺, 45), 1037 ([M - 7CO - 3CH₃]⁺, 30), 1024 ([M - 8CO - 2CH₃]⁺, 25), 1009 ([M - 8CO - 3CH₃]⁺, 21), 994 ([M - 8CO - 4CH₃]⁺, 20). Satisfactory analyses could not be obtained due to sample decomposition over days.

X-ray Crystallography. Crystals of compounds **2a**, **3a**, and **5a** suitable for diffraction analyses were grown by slow diffusion of methanol into either dichloromethane (**2a**, **3a**) or chloroform (**5a**) solutions at room temperature. Unique diffractometer data sets were measured at ~295 K within the specified 2θ_{max} limit (2θ/θ scan mode; monochromatic Mo *K*α radiation (λ = 0.71073 Å) yielding *N* independent reflections. *N*_o of these with *I* > 3σ(*I*) were considered "observed" and used in the full-matrix/large block least-squares refinements after analytical absorption correction. Anisotropic thermal parameters were refined for the non-hydrogen atoms; (*x*, *y*, *z*, *U*_{iso})_H were included, constrained at estimated values. Conventional residuals *R*, *R*_w on |*F*| at convergence are given. Neutral atom complex scattering factors were used, computation using the XTAL 3.2 program system (**2a**, **3a**),⁶ implemented by Hall, or teXsan (**5a**).⁷ Pertinent results are given in the figures and tables. Individual variants are noted in Table 1.

Results and Discussion

Syntheses and Characterization. The reactions of CpWIr₃(CO)₁₁ (**1**) with *n* equiv of PPh₃ (*n* = 1, 2, or 3) or PMe₃ (*n* = 1, 2, or 3) proceed in dichloromethane at room temperature to afford the clusters CpWIr₃(μ-CO)₃(CO)_{8-*n*}(PPh₃)_{*n*} (*n* = 1, **2**; *n* = 2, **3**; *n* = 3, **4**) or CpWIr₃(μ-CO)₃(CO)_{8-*n*}(PMe₃)_{*n*} (*n* = 1, **5**; *n* = 2, **6**; *n* = 3, **7**), respectively, as the major or sole reaction products in fair to excellent yields (38–63%). The products have been characterized by a combination of IR and ¹H, ¹³C, and ³¹P NMR spectroscopies, FAB MS, and satisfactory

(6) Hall, S. R.; Flack, H. D.; Stewart, J. M. *The Xtal 3.2 Reference Manual*; Universities of Western Australia, Geneva, and Maryland: Nedlands, Western Australia, Geneva, Switzerland, and College Park, MD, 1992.

(7) teXsan; *Single Crystal Structure Analysis Software, version 1.6c*; Molecular Structure Corp.: The Woodlands, TX, 1993.

(5) Complex **4** has been isolated and formulated previously: McAteer, C. H.; Shapley, J. R. Unpublished results.

Table 2. Important Bond Lengths (Å) for Complexes 2a and 3a

	2a	3a	2a	3a
Ir(1)–Ir(2)	2.6775(9)	2.708(3)	Ir(2)–C(21)	1.87(1)
Ir(1)–Ir(3)	2.734(1)	2.778(3)	Ir(2)–C(22)	1.87(1) 1.73(5)
Ir(2)–Ir(3)	2.685(1)	2.725(3)	Ir(3)–C(31)	1.94(1) 1.82(4)
Ir(1)–W(4)	2.813(1)	2.785(3)	Ir(3)–C(32)	1.92(1) 1.97(5)
Ir(2)–W(4)	2.841(1)	2.918(3)	Ir(3)–C(33)	1.90(1) 1.81(5)
Ir(3)–W(4)	2.896(1)	2.869(3)	W(4)–C(2)	2.09(1) 2.19(5)
Ir(1)–P(1)	2.330(3)	2.34(1)	W(4)–C(3)	2.17(1) 2.09(5)
Ir(2)–P(2)		2.32(1)	W(4)–C(41)	1.97(1) 1.88(4)
Ir(1)–C(1)	2.08(1)	2.12(4)	W(4)–C(01)	2.31(2) 2.29(5)
Ir(1)–C(3)	2.10(1)	2.04(4)	W(4)–C(02)	2.32(1) 2.24(7)
Ir(1)–C(11)	1.85(1)	1.74(5)	W(4)–C(03)	2.34(2) 2.30(7)
Ir(2)–C(1)	2.14(1)	2.00(4)	W(4)–C(04)	2.30(2) 2.26(5)
Ir(2)–C(2)	2.17(1)	2.09(5)	W(4)–C(05)	2.27(2) 2.23(5)

Table 3. Important Bond Lengths (Å) for Complex 5a

	mol A	mol B	mol C	mol D
Ir(1)–Ir(2)	2.756(1)	2.733(1)	2.734(1)	2.738(1)
Ir(1)–Ir(3)	2.739(1)	2.739(1)	2.748(1)	2.747(1)
Ir(2)–Ir(3)	2.753(2)	2.757(1)	2.750(1)	2.745(1)
Ir(1)–W(1)	2.855(1)	2.838(1)	2.846(1)	2.838(1)
Ir(2)–W(1)	2.839(1)	2.837(1)	2.836(1)	2.843(1)
Ir(3)–W(1)	2.894(1)	2.897(1)	2.886(1)	2.892(1)
Ir(3)–P(1)	2.312(7)	2.322(7)	2.313(7)	2.322(7)
Ir(1)–C(1)	2.10(2)	2.09(3)	2.10(2)	2.14(3)
Ir(1)–C(3)	2.13(2)	2.06(3)	2.10(3)	2.10(3)
Ir(1)–C(11)	1.85(2)	1.87(2)	1.94(3)	1.89(2)
Ir(1)–C(12)	1.93(3)	1.90(2)	1.92(2)	1.95(2)
Ir(2)–C(1)	2.12(2)	2.14(2)	2.11(3)	2.12(2)
Ir(2)–C(2)	2.13(3)	2.13(2)	2.13(2)	2.12(3)
Ir(2)–C(21)	1.81(3)	1.88(3)	1.93(3)	1.81(3)
Ir(2)–C(22)	1.94(2)	2.01(3)	1.95(2)	1.92(3)
Ir(3)–C(2)	2.11(2)	2.07(2)	2.06(2)	2.06(2)
Ir(3)–C(3)	2.12(2)	2.05(2)	2.09(2)	2.07(2)
Ir(3)–C(31)	1.81(3)	1.86(3)	1.87(3)	1.87(3)
W(1)–C(41)	1.98(2)	2.00(2)	1.96(3)	1.95(3)
W(1)–C(42)	1.99(3)	1.94(3)	1.99(2)	2.00(3)
W(1)–C(01)	2.30(2)	2.29(2)	2.29(3)	2.26(2)
W(1)–C(02)	2.28(2)	2.34(2)	2.31(2)	2.28(2)
W(1)–C(03)	2.38(3)	2.40(2)	2.36(3)	2.39(3)
W(1)–C(04)	2.41(3)	2.38(2)	2.37(2)	2.39(2)
W(1)–C(05)	2.31(3)	2.31(2)	2.32(2)	2.32(2)

microanalyses. Infrared spectra suggest the presence of edge-bridging carbonyl ligands in all complexes ($\nu(\text{CO})$ 1840–1807 cm^{-1}), which contrasts with the all-terminal precursor **1**. In combination with the X-ray structural results detailed below, the number of bands in the terminal carbonyl ligand $\nu(\text{CO})$ region is indicative of the presence of isomers. The ^1H and ^{13}C NMR (where appropriate) spectra contain signals assigned to Cp and Ph groups for **2–4**, and Cp and Me groups for **5–7**. Discussion of the ^{31}P NMR spectra is deferred until the solid state structures are presented (see below), but the spectra indicate the presence of interconverting isomers in solution; the crystallographically observed isomers of **2**, **3**, and **5** are labeled **a**. The FAB mass spectra of complexes **2**, **3**, and **5** have molecular ions, stepwise loss of carbonyls, and isotope patterns consistent with the presence of three iridium atoms and one tungsten atom; in some cases, loss of Ph is competitive with loss of the last few carbonyl ligands. The FAB mass spectra of derivatives **4**, **6**, and **7** do not contain molecular ions. Although mass spectra for **6** and **7** exhibit loss of carbonyls from the molecular ion, that of **4** shows initial loss of a phosphine ligand, followed by loss of carbonyls, possibly a result of steric factors.

X-ray Structural Studies of 2a, 3a, and 5a. The molecular structures of **2a**, **3a**, and **5a** as determined

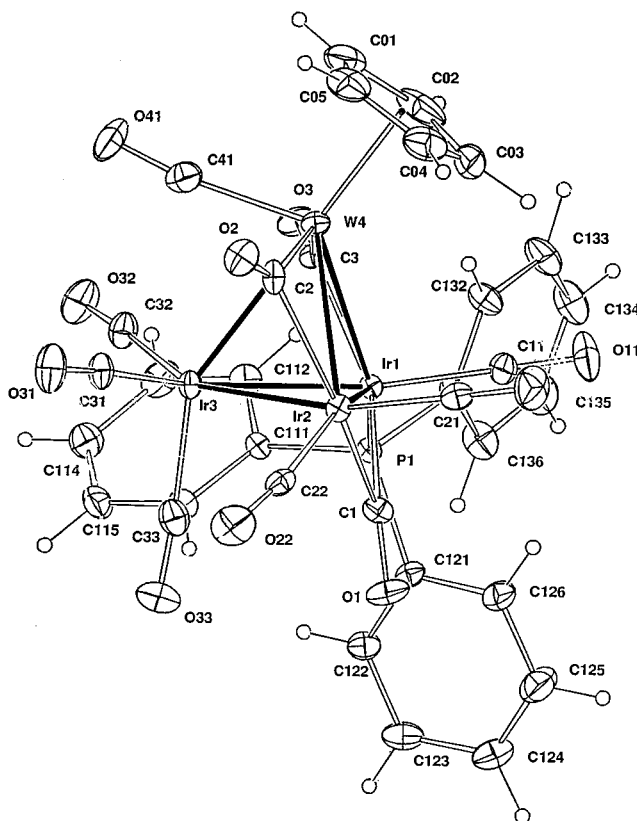


Figure 3. Molecular structure and atomic labeling scheme for $\text{CpWIr}_3(\mu\text{-CO})_3(\text{CO})_7(\text{PPh}_3)$, **2a**. Thermal envelopes of 20% probability are shown for the non-hydrogen atoms; hydrogen atoms have arbitrary radii of 0.1 Å.

by single-crystal X-ray studies are consistent with the formulations given above, define the substitution sites for these derivatives, and aid interpretation of the ^{31}P NMR spectra (see below). A summary of crystal and refinement data is found in Table 1, and selected bond distances are listed in Tables 2 (**2a** and **3a**) and 3 (**5a**). ORTEP plots showing the molecular geometry and atomic numbering scheme are shown in Figures 3 (**2a**), 4 (**3a**) and 5 (**5a**).

Complexes **2a** and **3a** have the WIr_3 pseudotetrahedral framework of the precursor cluster **1** and possess η^5 -cyclopentadienyl groups, three bridging carbonyls arranged about a WIr_2 plane, six (**3a**) or seven (**2a**) terminal carbonyl ligands, and one (**2a**) or two (**3a**) iridium-ligated triphenylphosphine ligands. The WIr_3 core distances ($\text{W}-\text{Ir}_{\text{av}} = 2.85$ Å, **2a**, and 2.86 Å, **3a**; $\text{Ir}-\text{Ir}_{\text{av}} = 2.699$ Å, **2a**, and 2.737 Å, **3a**) can be compared to those of **1** ($\text{W}-\text{Ir}_{\text{av}} = 2.82$ Å, $\text{Ir}-\text{Ir}_{\text{av}} = 2.699$ Å) and possibly suggest some slight core expansion; core distances of the diphosphine-substituted complexes $\text{CpWIr}_3(\mu\text{-dppe})(\mu\text{-CO})_3(\text{CO})_6$, $\text{CpWIr}_3(\mu\text{-dppm})(\mu\text{-CO})_3(\text{CO})_6$, and $\text{CpWIr}_3(\mu\text{-dppa})(\mu\text{-CO})_3(\text{CO})_6$ are also larger than those of **1**.¹ As previously observed in the diphosphine clusters, the longest $\text{W}-\text{Ir}$ distance in **2a** is effectively *trans* to the Cp group, although that in **3a** is on the WIr_2 face to which the Cp group is inclined. In **3a**, the shortest $\text{Ir}-\text{Ir}$ bonds are between the phosphine-coordinated iridiums, the longest $\text{Ir}-\text{Ir}$ vector in both $\text{CpWIr}_3(\mu\text{-dppe})(\mu\text{-CO})_3(\text{CO})_6$ and $\text{CpWIr}_3(\mu\text{-dppm})(\mu\text{-CO})_3(\text{CO})_6$. The cyclopentadienyl groups in **2a** and **3a** are inclined toward the WIr_2 faces containing the bridging carbonyl ligands. Carbonyl distances and angles for **3a** are relatively imprecise and will not be

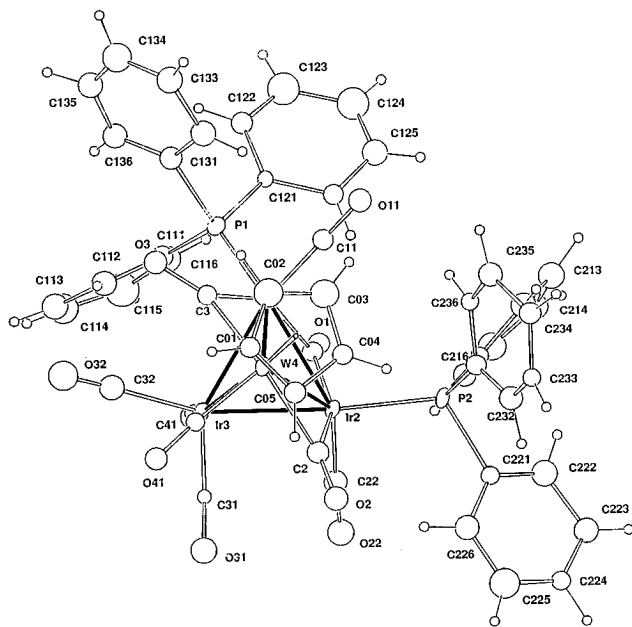


Figure 4. Molecular structure and atomic labeling scheme for $\text{CpWIr}_3(\mu\text{-CO})_3(\text{CO})_6(\text{PPh}_3)_2$, **3a**. Thermal envelopes of 20% probability are shown for the non-hydrogen atoms; hydrogen atoms have arbitrary radii of 0.1 Å.

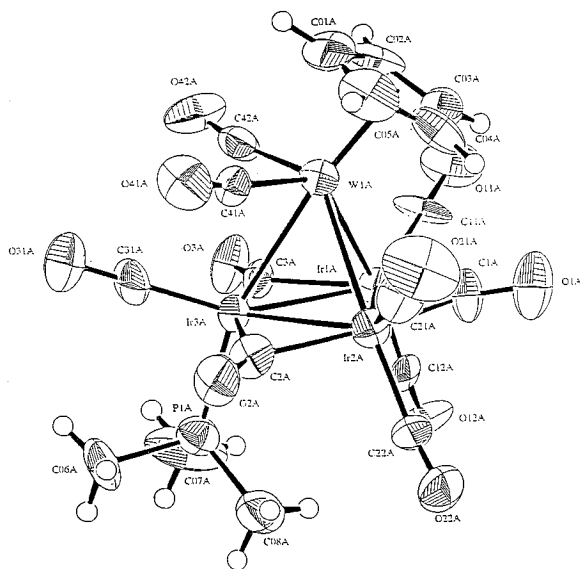


Figure 5. Molecular structure and atomic labeling scheme for $\text{CpWIr}_3(\mu\text{-CO})_3(\text{CO})_7(\text{PMe}_3)_3$, **5a**. Thermal envelopes of 50% probability are shown for the non-hydrogen atoms; hydrogen atoms have arbitrary radii of 0.1 Å.

discussed here. Ir–CO(terminal) interactions for **2a** (1.85(1)–1.94(1) Å) and W–CO(terminal) distances (1.97(1) Å) are comparable to those reported in other tungsten–iridium carbonyl complexes;^{4,8} the M–C–O angles are in the normal range for terminal carbonyl groups (171(1)–178(1)°). In **2**, carbonyls 1 and 3 bridge asymmetrically toward Ir(1), with Ir(1)–CO(1) 2.08(1) Å, Ir(2)–CO(1) 2.14(1) Å, Ir(1)–CO(3) 2.10(1) Å, and W(4)–CO(3) 2.17(1) Å; CO(2) is displaced toward tungsten [W(4)–CO(2) 2.09(1) Å, Ir(2)–CO(2) 2.17(1) Å]. The asymmetry in bridging carbonyls presumably reflects

the increase in electron density (and capacity for back-donation) at Ir(1) resultant upon phosphine substitution. Complexes **2a** and **3a** are the first examples from the tungsten–iridium system with bridging carbonyls at a WIr_2 face. The Ir–P distances (2.330(3) Å (**2a**), 2.33 Å (**3a**) (average)) are unexceptional, as are the intraphosphine bond lengths and angles. Formal electron counting reveals that **2a** and **3a** have 60 e, electron precise for tetrahedral clusters.

Single-crystal X-ray diffraction of **5a** revealed the presence of four independent molecules per asymmetric unit, each molecule differing only slightly from the others. No chemically significant differences exist in the four independent molecules; a representative molecule is depicted in Figure 5. As with **2a**, complex **5a** also possesses a WIr_3 pseudotetrahedral framework with η^5 -cyclopentadienyl groups, phosphine ligand, and seven terminal carbonyl ligands but instead has three bridging carbonyls arranged around the triiridium plane, a structural type found previously with the bidentate ligand derivatives $\text{CpWIr}_3(\mu\text{-L})(\mu\text{-CO})_3(\text{CO})_6$ (L = dpmm, dppe, dppa).¹ The WIr_3 core distances (W–Ir_{av} 2.863 Å, Ir–Ir_{av} 2.749 Å) are comparable to **2a** and **3a**; as with **2a**, the longest W–Ir distance for **5a** is effectively *trans* to the Cp group, and the shortest Ir–Ir bond is that effectively *trans* to the phosphine ligand. The cyclopentadienyl group is inclined toward a WIr_2 face; three W–C distances (average 2.30 Å) are shorter than the two W–C distances (average 2.40 Å) involving the carbons closest to the Ir–Ir vector. Ir–CO(terminal) interactions (1.81(5)–1.94(1) Å) and W–CO interactions (1.98(2)–1.99(3) Å) are normal. Cluster **5a** is also electron precise with 60 e.

Discussion. As mentioned above, the IR spectra in the terminal carbonyl ligand $\nu(\text{CO})$ region are indicative of the presence of isomers. This is also true of the ³¹P NMR spectra. The room-temperature ³¹P NMR spectrum of **2** contains a broad resonance at about –0.5 ppm, which decoalesces to give resonances (ratio approximately 4:5) at 4.7 and –5.1 ppm at 228 K. Similarly, the room-temperature spectrum of **3** contains two broad resonances, which sharpen on cooling to 230 K to give three resonances at 27.3, 25.1, and –7.7 ppm in the ratio 2:1:1. The room-temperature ³¹P NMR spectra of the complexes **4**–**7** were found to have either broad resonances or no signals at all. Lowering the temperature to 230 K sharpened the resonances, suggesting fluxionality in each of the derivatives. In analogous tetrairidium clusters, Shapley has assigned downfield ³¹P NMR resonances to radially-coordinated phosphines and upfield signals to axially-coordinated phosphines, with respect to the plane of the bridging carbonyl ligands.⁹ This has been generalized and extended; in the ¹H, ¹³C, and ³¹P NMR spectra of tetrairidium cluster compounds, the chemical shifts of the ligands decrease in the following positional sequence: bridging > radial > axial ≈ apical.^{10a} Resonances of the phosphine-substituted tungsten–iridium clusters, and their suggested sites of substitution, are listed in Table 4. As detailed below, these substitution sites have been assigned by utilizing information from (a) the crystallographically-verified isomers, (b) the substitution pattern in the tetrairidium system (see Introduction), and (c) chemical shifts in the ³¹P NMR spectra.

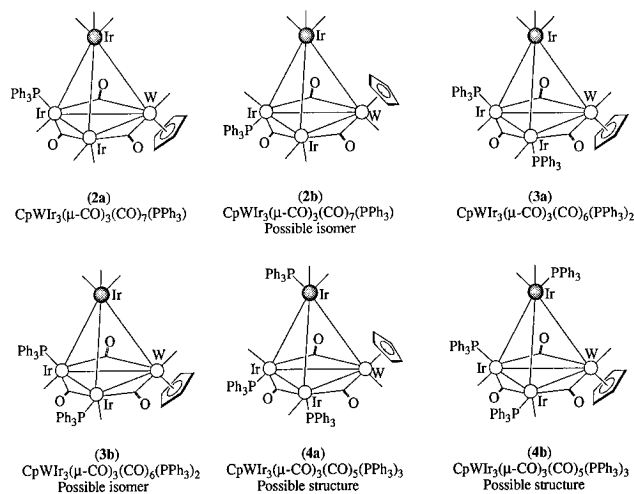
(8) (a) Churchill, M. R.; Bueno, C.; Hutchinson, J. P. *Inorg. Chem.* **1982**, *21*, 1359. (b) Churchill, M. R.; Biondi, L. V. *J. Organomet. Chem.* **1989**, *366*, 265. (c) Churchill, M. R. *J. Organomet. Chem.* **1985**, *280*, C63.

(9) Stuntz, G. F.; Shapley, J. R. *J. Am. Chem. Soc.* **1976**, *99*, 607.

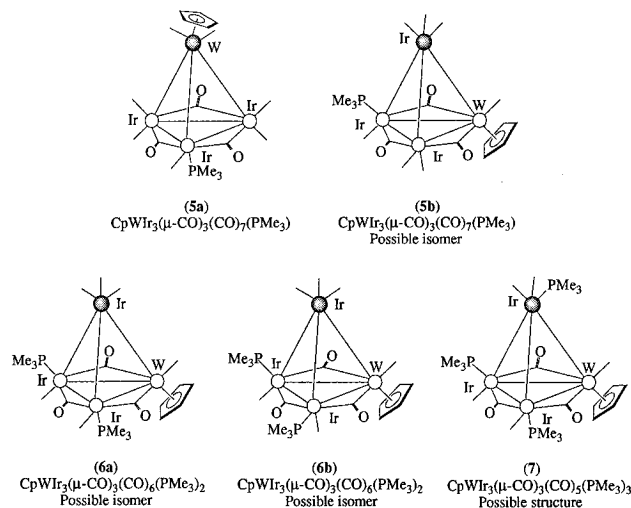
Table 4. ^{31}P NMR Data for $\text{CpWIr}_3(\mu\text{-CO})_3(\text{CO})_{11-x}(\text{PR}_3)_x$ ($\text{R} = \text{Ph, Me; } x = 1, 2, \text{ or } 3$)

complex	^{31}P NMR chem shifts	suggested site of PR_3 substitution, with respect to $(\mu\text{-CO})_3$ plane	isomer ratio
$n = 1, \text{R} = \text{PPh}_3$	2a 4.7 ^a	radial ^c	4
	2b -5.1 ^a	axial	5
$n = 2, \text{R} = \text{PPh}_3$	3a 25.1, -7.7 (1:1) ^a	radial, axial ^c	1
	3b 27.3 ^a	diradial	1
$n = 3, \text{R} = \text{PPh}_3$	4a 31.8, -17.9 (2:1) ^a	diaxial, apical	
	4b	diradial, apical	
$n = 1, \text{R} = \text{PMe}_3$	5a -30.2 ^b	axial ^c	3
	5b -26.1 ^b	radial	2
$n = 2, \text{R} = \text{PMe}_3$	6a -22.7, -38.7 (1:1) ^b	radial, axial	4
	6b -20.8 ^b	diradial	5
$n = 3, \text{R} = \text{PMe}_3$	7 -27.1, -45.2, -83.4 (1:1:1) ^b	radial, axial, apical	

^a CDCl_3 , 230 K. ^b Acetone- d_6 , 230 K. ^c Crystallographically confirmed.

**Figure 6.** Possible configurations for **2–4**.

Geometries of possible isomers of **2–4** are given in Figure 6. The crystallographically observed **2a** has Cp occupying an axial site and PPh_3 occupying a radial site (radial, axial isomer). The axially coordinated phosphine is consistent with the other isomer adopting diaxial or radial, axial geometries, but we favor the latter (**2b**); diaxial coordination is unlikely with bulky ligands (cone angles: Cp 136° , PPh_3 145°). Isomer **3a** is the crystallographically observed radial, diaxial form. The other isomer presumably adopts the diradial, axial structure **3b**, which would minimize steric repulsion from the Cp ligand. All previous structurally confirmed tetrasubstituted tetrahedral tetrairidium clusters adopt radial, diaxial, apical geometries.^{9,10bc} Assuming that this substitution pattern (which minimizes steric repulsion) is maintained, a signal of intensity 2 downfield of a signal of intensity 1 suggests that the phosphines are located at axial and apical sites in **4a**, with the Cp in a radial position. The alternative, consistent with the chemical shift data, but involving a new tetrasubstituted coordination geometry, is for the phosphines to occupy diradial, apical sites as in **4b**. Structure **4b** involves greater steric repulsion of phosphine ligands than that in the ideal tetrasubstituted radial, diaxial, apical geometry; consistent with assignment as structure **4b** is that **4** (i) loses phosphine in solution over hours (which has precluded an X-ray structural study) and (ii) does not have a molecular ion in the FAB MS but rather $[\text{M} - \text{PPh}_3]^+$.

**Figure 7.** Possible configurations for **5–7**.

Isomer assignment requires a crystallographic underpinning to be solid; the suggested geometries of trimethylphosphine derivatives are necessarily cautious, given that only one crystallographically verified example exists. Geometries of possible isomers of **5–7** are displayed in Figure 7. Isomer **5a** is the crystallographically observed form, with an axial PMe_3 . Considering the Cp coordination site also, it is a disubstituted cluster of axial, apical geometry. Only *trans* axial, apical geometries as in **5a** have been crystallographically confirmed,¹¹ a *cis* axial apical isomer is conceivable, but the observation of only one ^{31}P NMR resonance for diaxially-coordinated diphosphine clusters $\text{CpWIr}_3(\mu\text{-L})(\mu\text{-CO})_3(\text{CO})_6$ ($\text{L} = \text{dppe, dppm}$) where the crystal structure shows ligated *P* both *trans* and *cis* to the apical Cp suggests that $\text{CpW}(\text{CO})_2$ tripodal rotation is rapid in solution and that such *trans* and *cis* isomers are indistinguishable on the NMR timescale. Alternative **5b**, with a carbonyl-bridged WIr_2 face as in the triphenylphosphine complexes above, is most probable; the radial, axial form as drawn minimizes phosphine cyclopentadienyl repulsion. The combination of ^{31}P NMR shifts observed for **6** and **7** and tri- and tetrasubstituted geometries structurally characterized in previous work with tetrahedral clusters lead us to postulate geometries **6a**, **6b**, and **7**. Trisubstituted geometries are invariably radial, diaxial or diradial, axial; NMR data are consistent with **6a** adopting the former and **6b** the latter geometries. NMR data for **7** combined with the previously characterized radial, diaxial, apical geometries for

(10) (a) Ros, R.; Scrivanti, A.; Albano, V. G.; Braga, D. *J. Chem. Soc., Dalton Trans.* **1986**, 2411. (b) Darensbourg, D. J.; Baldwin-Zuschke, B. J. *Inorg. Chem.* **1981**, *20*, 3846. (c) Blake, A. J.; Osborne, A. G. *J. Organomet. Chem.* **1984**, *260*, 227.

(11) Keller, E.; Vahrenkamp, H. *Chem. Ber.* **1981**, *114*, 1111.

tetrasubstitution are only consistent with the radial, axial, apical assignment displayed. Clearly, further structural data for phosphine-substituted tungsten–iridium clusters are needed to support these tentative assignments; in particular, the isolation and structural characterization of clusters with Ir₃ and WIr₂ edge-bridged faces suggests that the assignments above should be treated with caution. The ³¹P NMR data support WIr₂-edge bridged geometries for **6** and **7**; the possibility therefore exists that the crystallographically verified **5a** is a minor isomer not observed in the ³¹P NMR and that the resonance at –30.2 ppm is from an analogue of **2b** with a WIr₂-edge bridged structure.

Our investigations extend previous work on ligand substitution at tetrairidium clusters and structural studies on the resultant species^{10,12} into the mixed-metal domain. Replacement of Ir(CO)₃ by isolobal CpW(CO)₂ in the tetrahedral core immediately introduces possible isomers in the carbonyl-bridged form; the Cp ligand can

occupy axial, radial or apical sites, and we have now structurally characterized examples of the axial and apical forms, although the radial has thus far proved elusive.

Related structurally-characterized mixed-metal clusters containing one metal from group 6 and three metals from group 9 in the carbonyl-bridged form, i.e. CpMoCo₃(μ-CO)₃(CO)₈¹³ and CpMoIr₃(μ-CO)₃(CO)₈,¹⁴ have the basal plane containing the lighter metals, i.e. Co₃(μ-CO)₃ for the former, MoIr₂(μ-CO)₃ for the latter. Neither tungsten nor iridium favor the carbonyl-bridged geometry (which in general becomes increasingly less likely on descending a group); as a consequence, both WIr₂(μ-CO)₃ and Ir₃(μ-CO)₃ basal planes are accessible in this system. Although CpWIr₃(CO)₁₁ adopts the all-terminal geometry in the solid state,⁴ its ¹³C NMR spectrum (169.2 ppm (11 CO)) suggests carbonyl exchange over all positions, presumably by way of bridged intermediates.¹⁴ The present investigation provides examples of edge-bridging species as putative models for carbonyl scrambling intermediates in CpWIr₃(CO)₁₁.

Acknowledgment. We thank the Australian Research Council for support of this work and Johnson-Matthey Technology Centre for the loan of IrCl₃. M.G.H. is an ARC Australian Research Fellow.

Supporting Information Available: Tables giving final values of all refined atomic coordinates, all calculated atomic coordinates, all anisotropic and isotropic thermal parameters, and all bond lengths and angles (100 pages). Ordering information is given on any current masthead page.

OM950554O

(12) (a) Tranqui, D.; Durif, A.; Nasr Eddine, M. *Acta Crystallogr.* **1982**, *B38*, 1920. (b) Strawczynski, A.; Ros, R.; Roulet, R.; Braga, D.; Gradella, C.; Grepioni, F. *Inorg. Chim. Acta* **1990**, *170*, 17. (c) Flörke, U.; Haupt, H.-J. *Z. Kristallogr.* **1990**, *191*, 149. (d) Clucas, J. A.; Harding, M. M.; Nicholls, B. S.; Smith, A. K. *J. Chem. Soc., Chem. Commun.* **1984**, 319. (e) Albano, V.; Bellon, P.; Scatturin, V. *Chem. Commun.* **1967**, 730. (f) Strawczynski, A.; Ros, R.; Roulet, R. *Helv. Chim. Acta* **1988**, *71*, 867. (g) Albano, V. G.; Braga, D.; Ros, R.; Scrivanti, A. *J. Chem. Soc., Chem. Commun.* **1985**, 866. (h) Braga, D.; Grepioni, F.; Guadalupi, G.; Scrivanti, A.; Ros, R.; Roulet, R. *Organometallics* **1987**, *6*, 56. (i) Shapley, J. R.; Stuntz, G. F.; Churchill, M. R.; Hutchinson, J. P. *J. Am. Chem. Soc.* **1979**, *101*, 7425. (j) Churchill, M. R.; Hutchinson, J. P. *Inorg. Chem.* **1979**, *18*, 2451.

(13) Schmidt, G.; Bartl, K.; Boese, R. *Z. Naturforsch. B* **1977**, *32*, 1277.

(14) Churchill, M. R. *J. Organomet. Chem.* **1986**, *312*, 121.